A Microconcentric Ring Electrode/Injector Assembly for Sensitive Voltammetric Analysis in Single Droplets of Ultrasmall Volumes.

ARTICLE *in* ANALYTICAL CHEMISTRY · JULY 2014

Impact Factor: 5.64 · DOI: 10.1021/ac502316p · Source: PubMed

5 AUTHORS, INCLUDING:

Tianhan Kai
California State University, Los Angeles
6 PUBLICATIONS **4** CITATIONS
SEE PROFILE

Shu Chen
Hunan University of Science and Technology
33 PUBLICATIONS **203** CITATIONS
SEE PROFILE

Estuardo Monterroso
California State University, Los Angeles
2 PUBLICATIONS **1** CITATION
SEE PROFILE

Feimeng Zhou
California State University, Los Angeles
136 PUBLICATIONS **4,810** CITATIONS
SEE PROFILE

analytical chemistry

Technical Note

pubs.acs.org/ac

Microconcentric Ring Electrode/Injector Assembly for Sensitive Voltammetric Analysis in Single Droplets of Ultrasmall Volumes

Tianhan Kai,[†] Shu Chen,[†] Estuardo Monterroso,[‡] Amanuel Hailu,[‡] and Feimeng Zhou*[,‡]

[†]College of Chemistry and Chemical Engineering, Central South University, Changsha, Hunan P. R. China 410083

[‡]Department of Chemistry and Biochemistry, California State University, Los Angeles, Los Angeles, California 90032, United States

Supporting Information

ABSTRACT: This paper describes the construction of a microring electrode concentric to an inner injection capillary for voltammetric determination of trace analytes in nanoliter- to picoliter-sized droplets. The gold microring is sandwiched between a pulled fused-silica capillary and borosilicate glass tubing. Compared to polymer-coated microring electrodes, the glass-encapsulated electrode is more robust and does not swell in organic solvents. Consequently, the microring electrode is suitable for voltammetric studies of redox-active species and their accompanying ion transfers between two immiscible solvents. Droplets of variable sizes can be conveniently dispensed from front-loaded sample plugs into an immiscible liquid, greatly simplifying the experimental procedure and facilitating analysis of samples of limited availability. The size of the microring and the volume of the droplet deduced from well-defined voltammograms correlate well with those estimated from their geometric dimensions. The thin-layer cell behavior can be attained with well-defined voltammetric peaks and small capacitive current. Exhaustive electrolysis in single droplets can be accomplished in short times (e.g., ~85 s in a droplet of 1.42 nL at a microring of 11.4 μm in radius). Anodic stripping voltammetry of Ag deposited onto the microring electrode resulted in a detection limit of 0.13 fmol (14 fg) of Ag^+. The microring electrode/injector assembly can be polished repeatedly and is versatile for various applications (e.g., sample plugs can also be back-loaded via a rotary injection valve and an HPLC pump for flow injection analysis).

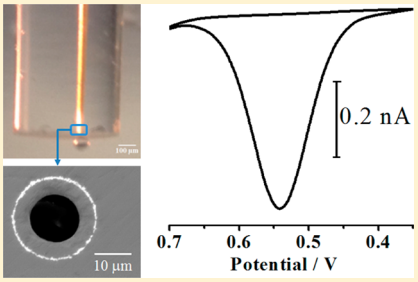

Since late 1980s, electrochemists and electroanalytical chemists alike have witnessed the meteoric rise of microelectrodes and the rapid expansion of their applications.[1−3] The prominent features of microelectrodes, compared to conventional-sized electrodes (e.g., disc electrodes with diameters greater than 25 μm),[2] include the substantially reduced "ohmic (iR) drop" and double-layer capacitance, significantly enhanced mass transfer rates, and drastically improved signal-to-noise ratios. Studies of electrode reactions and surface-bound molecules with high temporal[4] and spatial resolution[5] or in exotic (e.g., highly resistive) media have become possible.[2,6]

Another advantage of microelectrodes is that measurements can be made on incredibly small specimens or in extremely small volumes. As mentioned by Bond,[2] the consideration of using a microelectrode to measure oxygen in muscle tissue, perhaps the earliest application of microelectrode,[7] was to minimize the damage to the muscle with a small electrode. Nowadays, investigations on chemical reactions and biological events at single cells are commonplace.[4,8−11] A well-known example is the measurement of exocytosis of neurotransmitters of individual neurons.[12,13] Microdisc and microband electrodes have also been employed by many others[14−18] to measure samples of volumes ranging from microliters to even attoliters.

A potentially simpler and more cost-effective approach is to conduct electrochemical analysis in an exceedingly small solution surrounded by an immiscible liquid. An attractive aspect of this approach is that the immiscible liquid prevents the analyte solution from rapid evaporation. Wei et al. showed that a thin-layer of aqueous solution can be brought along with a scanning electrochemical microscopic (SECM) tip as it moved into a nonaqueous (e.g., nitrobenzene or NB) phase.[19] Using a micromanipulator and operating under a microscope, Kitamura and co-workers injected a picoliter-sized NB droplet onto an inverted gold microelectrode and studied the distribution of a ferrocene derivative between NB and water phases.[20] They also trapped a single NB droplet with a laser onto a carbon fiber electrode.[21] Recently, Yum et al. inserted a carbon nanotube into an aqueous droplet submerged under mineral oil.[22] The above-mentioned methods all require a micromanipulator system for positioning the droplets or microelectrodes, and the complicated procedure is therefore not suitable for high-throughput analyses.

Ion transfer reactions between two immiscible liquids have been extensively interrogated electrochemically.[23−26] However, the approach is not amenable for studies of redox reactions of electroactive species or voltammetric detection of analytes at trace levels. If small droplets confined by an immiscible liquid are also exposed to a microelectrode, the high mass transfer rate in small volumes should lead to rapid and exhaustive

Received: June 17, 2014
Accepted: July 27, 2014
Published: July 28, 2014

   dx.doi.org/10.1021/ac502316p | *Anal. Chem.* 2014, 86, 8037−8041

electrolysis and hence low analyte detection limits. One approach is therefore to fabricate a microring electrode that is concentric to a micropipet-like injector. Given the high perimeter-to-area ratio of microring electrodes, the mass transfer or electrolytic rate should be even greater than those attainable at microdisc electrodes.[27,28] Indeed, Macpherson and Unwin have developed a radial flow microring electrode (RFMRE), which is a thin Pt film coated onto the outer wall of a capillary nozzle and sealed with epoxy resin.[29] When this RFMRE (66 μm in radius) was positioned close to a planar substrate using a micropositioner, the extremely high mass transfer rates facilitated the measurements of rapid heterogeneous electron-transfer kinetics.[30,31] Bard and co-workers sealed a much smaller microring (~1.3 μm in radius) with electrophoretic paint and employed it as a tip for SECM imaging in the generation/collection mode.[32] Such a microring tip holds the promise of delivering solutions during the SECM imaging to obtain additional chemical information about the surface. Although in principle both types of microring electrodes should allow single droplets to adhere to the microring electrode, the polymeric materials used to seal these microring electrodes can swell in organic solvents, resulting in leakage or much increased charging current. Moreover, the electrode is either too fragile for routine analysis or too large in diameter for reducing the size of the droplet.

We report here the fabrication and characterization of a microring Au electrode (radius variable between 5 and 25 μm) sandwiched between a pulled fused-silica capillary and borosilicate glass tubing. The tight seal by boroslicate glass tubing benefitted from coating the entire tapered portion of the capillary with a uniform Au film. The resultant microring electrode/injector assembly is chemically inert as it does not swell in organic solvents or erode in caustic solutions. It is also rugged and can be polished repeatedly. Extremely small sample solution can be front-loaded and subsequently suspended in an immiscible liquid. We demonstrate that exhaustive electrolysis in single droplets can be achieved in a single voltammetric scan or within a short time in controlled potential electrolysis, facilitating rapid analysis of exceedingly low quantities of analytes. This microconcentric ring/injector assembly obviates the use of a micromanipulator system, shortens analysis time, and drastically reduces the sample consumption.

EXPERIMENTAL SECTION

Chemicals. Ruthenium hexamine chloride ($Ru(NH_3)_6Cl_3$), ferrocene (Fc), tetrabutylammonium chloride (TBACl), tetrabutylammonium tetraphenylborate (TBATPB), tetrabutylammonium perchlorate ($TBAClO_4$), $MgSO_4$, $AgNO_3$, KCl, and KNO_3 (Sigma-Aldrich, St. Louis, MO) and nitrobenzene (Fisher Scientific, Pittsburgh, PA) were used as received. Aqueous solutions were prepared with deionized water (18.2 MΩ cm^{-1}; Simplicity 185, Millipore Corp, Billerica, MA).

Electrode Fabrication. Fused-silica capillaries with polyimide coating (o.d. 363 ± 10 μm/i.d. 180 ± 6 μm) were obtained from Polymicro Technologies (Phoenix, AZ). They were pulled by a laser micropipet puller (P-2000, Sutter Instruments, Novato, CA) after a portion of the polyimide coating was removed in a flame. The typical parameters for the puller were HEAT = 450, Filament = 0, Velocity = 55, Delay = 132, and Pull = 0. The laser heating time was about 2 s, and the taper of the pulled capillaries was ~5 mm in length. To coat the pulled capillaries with a thin gold film, they were affixed to small aluminum square blocks with heat-resistant double-sided tape, which were then mounted with the capillaries parallel to the turntable into a thermal evaporator (model TBB-IV, Denton Vacuum Inc., Moorestown, NJ). The turntable was rotated at 45 rpm and positioned about 10 cm above the gold target. In each coating cycle, 105 mA was used to evaporate the gold target. Four coating cycles were performed with the aluminum blocks flipped 90° clockwise in between. The gold-coated taper of each capillary was carefully sealed into a borosilicate glass tubing (o.d. 1.2 mm/i.d. 0.69 mm, Sutter Instrument Co.) inside a heating coil under vacuum. Caution must be exercised to ensure that the gold film is not melted during the sealing process. Electrical contact was made by connecting a copper wire to the gold film on the side of capillary with silver epoxy (Epoxy Technology, Billerica, MA). The end of the encapsulating glass bulb was removed with coarse sandpaper. Subsequently, the microring was polished successively with 45, 15, 3, and 1 μm diamond abrasive plates on a microelectrode beveller (model BV-10, Buehler, Lake Bluff, IL). To avoid clogging the capillary with polishing materials or small broken glass pieces, polishing was carried out with pressurized air applied from the top of the capillary.

Instrument. All electrochemical experiments were measured with a CHI440 Electrochemical Analyzer (CH Instruments, Austin, TX). The microring electrode was the working electrode, and a Ag/AgCl electrode and a Pt wire served as the reference and auxiliary electrodes, respectively. When water droplets were dispensed into NB, a salt bridge containing saturated KNO_3 solution was used to prevent contamination of the Ag/AgCl electrode by NB.

Procedures. *Dispensing of Single Droplets.* To produce small droplets of picoliter volumes, the back of each microring electrode/injector assembly was connected to a microinjector (Sutter Instruments Inc.). The front end of the assembly was then vertically lowered into a sample solution with a positive air pressure applied from the back by the microinjector. A small amount of sample can thus be front-loaded and regulated by controlling the height of electrode assembly immersed in the solution (i.e., the amount of withdrawing capillary force) and the "inject" gas pressure applied (i.e., the extent of dispensing force). With the gas pressure maintained, the microring electrode assembly was raised out of the sample solution and transferred into an immiscible liquid. By gradually increasing the "inject" gas pressure of the microinjector, the solution inside the capillary was gently and completely pushed out as a droplet that adhered to the end of the electrode assembly. Droplet creation can be visualized with a telemicroscope (model BM 40018, Meiji Techno Co., Santa Clara, CA). To record votammograms of Fc in NB droplets, 10 mM TBATPB and 1.25 mM Fc were dissolved in NB, and the NB droplets were surrounded by aqueous solution containing 10 mM $MgSO_4$ and 1 mM TBACl. For anodic stripping analysis of Ag^+, aqueous solutions containing 10 mM KNO_3/10 mM HNO_3 and various $AgNO_3$ concentrations were dispensed into an NB solution containing 10 mM $TBAClO_4$.

Flow Injection Analysis. Samples can also be back-loaded and analyzed in the flow-injection mode. The back of the capillary was connected to a six-port rotary valve (Valco Inc., Houston, TX) with tubing sleeves and fingertight PEEK fittings (Upchurch Scientific, Oak Harbor, WA). With the front end of the capillary immersed in a small beaker housing an electrolyte solution and the reference and auxiliary electrodes, a carrier (0.1 M KCl) solution was continuously delivered by an HPLC pump (L-6000, Hitachi, Japan). Injections of $Ru(NH_3)_6Cl_3$ (5.0

dx.doi.org/10.1021/ac502316p | Anal. Chem. 2014, 86, 8037−8041

mM in 0.1 M KCl) preloaded into a 20-μL loop were monitored amperometrically.

RESULTS AND DISCUSSION

Figure 1A shows the detail of the microconcentric ring electrode/injector assembly. Removal of the bulb formed during the sealing process (bottom of Figure 1A) produces a gold microring that is concentric to the inner capillary. The ring size (R) and the capillary opening can be systematically varied by removing different lengths of the glass bulb. We were able to fabricate microring electrodes with a radius ranging from 5 μm (with the capillary opening of ~2.5 μm in radius) to 25 μm (with the capillary opening of ~12.5 μm in radius). Such controllability, similar to that in the approach developed by Macpherson and Unwin,[29] facilitates the construction of microring electrodes of variable dimensions for different applications. However, the radius of our microring electrode is much smaller, allowing ultrasmall droplets to be created and analyzed. Figure 1B is an SEM image of a microring electrode with a radius of 11.4 μm and a capillary opening (radius = 6.1 μm). The thickness of the gold ring is about 0.6 μm. Apparently, coating the Au film onto the tapered capillary wall side-on (cf. the Experimental Section), instead of end-on or at a tilted angle,[32,33] allows the entire tapered capillary to be coated with a smooth Au film for a better seal and easier electrical connection.

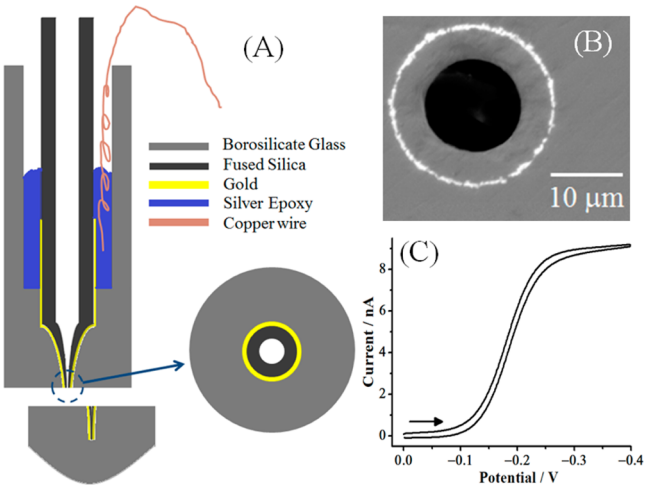

Figure 1. (A) Construction of the microconcentric ring electrode/injector. (B) An SEM image of the end of an exposed microring and the capillary opening. The ring is 11.4 μm in radius and the capillary has a radius of 6.1 μm. (C) Cyclic voltammogram of 5 mM $Ru(NH_3)_6^{3+}$ in 0.1 M KCl at the microring electrode. The scan rate was 20 mV/s, and the arrow indicates the initial scan direction.

The tight seal was also confirmed by cyclic voltammetry (Figure 1C). The sigmoidal voltammogram is indicative of a hemispherical diffusion of $Ru(NH_3)_6^{3+}$ to the electrode.[34] The theoretical equation for the steady-state current (i) at the microring electrode can be deduced by eq 1 and other equations.[28,35]

$$i = nFDc[\pi^2(a + b)]/\ln[16(a + b)/(b - a)] \quad (b/a < 1.25) \qquad (1)$$

where n is the number of electron transferred, F the Faraday constant, D the diffusion coefficient (0.53×10^{-5} cm^2/s), c the analyte concentration, a the inner ring radius (10.8 μm), and b the outer ring radius (11.4 μm). The limiting current was calculated to be 8.75 nA, which agrees extremely well with that assessed with cyclic voltammetry (8.86 nA).

The microring electrode can be readily connected to a microcapillary injection system driven by pressurized gas for controllably creating single droplets of volumes ranging from nano- to picoliters. To gain a better understanding about the voltammetric behavior, a small NB droplet was suspended in water (V = 96.5 pL deduced from the photomicrograph in Figure 2 based on the droplet width and height). At 10 mV/s, peaks were observed and the peak current (i_p) values decrease precipitously with scan cycles (Figure S1 in Supporting Information). At 2 mV/s (Figure 2), the first voltammetric scan produced a symmetric peak and the second peak did not show any Fc oxidation current. Our results are similar to those obtained by Kitamura and co-workers from a single NB droplet positioned onto an inverted microdisc electrode.[20] The voltammetric behavior is also the same as that in a thin-layer electrochemical cell, with exhaustive electrolysis achievable in a single scan. In a larger droplet (e.g., ~1.73 nL), sigmoidal curves, instead of peaked ones, were observed (Figure S2 in the Supporting Information). The continuous decrease in the steady-state currents suggests that Fc concentration in the droplet has gradually decreased. Considering the high distribution coefficient of Fc (K^{Fc} = [Fc(NB)]/[Fc(water)] = 7.0×10^3) between the NB and water phases,[36] the decrease cannot be ascribed to the loss of neutral Fc molecules. Analogous to other reports,[20,36] the decrease can be rationalized by the gradual loss of Fc^+ ions from NB to water. Although diffusion of anions (Cl^-) into and cations (TBA^+) out of the NB droplet could also help counterbalance the positive charges on the newly electrogenerated Fc^+, these processes are much less favorable than the diffusion of Fc^+ out of the NB droplet. This is conceivable given the greater solubility of Cl^- in water and higher solubility of TBA^+ in NB. This contention is also consistent with the small distribution coefficient of Fc^+ (K^{Fc+} = [Fc^+(NB)]/[Fc^+(water)] = 20) between the two immiscible phases.[36]

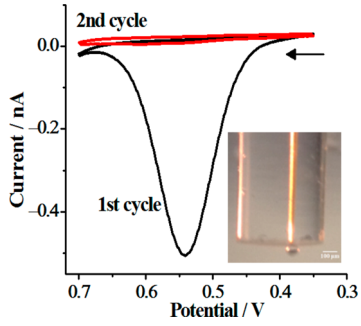

Figure 2. Continuous cyclic voltammetric scans in an NB droplet containing 1.25 mM Fc at 2 mV/s. The inset is a photomicrograph of the droplet with a width of 42.1 μm and height of 49.2 μm.

It is worth mentioning that, in a thin-layer electrochemical cell housing a conventional-sized working electrode, capacitive current and uncompensated iR drop become serious when nonaqueous solutions are used.[34] The small electrode size of our microring electrode reduced both the iR drop and capacitive current, as evidenced by the well-defined voltam-

dx.doi.org/10.1021/ac502316p | Anal. Chem. 2014, 86, 8037−8041

metric peak in Figure 2. The volume of the droplet (V) can also be calculated with the data in Figure 2 using Faraday's law:

$$Q = nFVC_{Fc} \quad (2)$$

where Q is the total charge under the oxidation peak. From the total charge (10.73 nC), the droplet volume was calculated to be 89 pL. This value is more accurate than that deduced from the photomicrograph in Figure 2 (96.5 pL), as the latter is subject to uncertainties in measuring the width and height of a small droplet.

Given that exhaustive electrolysis can be rapidly accomplished in a small droplet, we explored the analytical utility of our electrode for anodic stripping voltammetry (ASV) in a water droplet. When a small water droplet was dispensed into NB, a spherical cap (cf. inset of Figure 3A), instead of a dome,

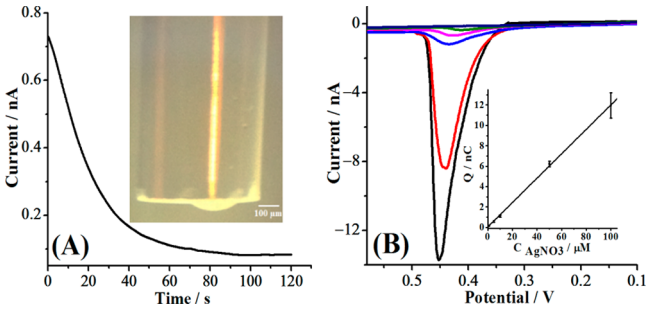

Figure 3. (A) Chronoamperomgram of 100 μM $AgNO_3$ in an aqueous droplet containing 10 mM KNO_3 and 10 mM HNO_3. The inset is a photomicrograph of a droplet surrounded by NB containing 10 mM $TBAClO_4$. (B) Anodic stripping voltammograms recorded after controlled potential deposition (0.000 V vs Ag/AgCl) for 100 s in droplets containing 0 (navy), 1 (green), 5 (magenta), 10 (blue), 50 (red), and 100 μM (black curve) $AgNO_3$. The scan rate was 50 mV/s. The inset shows the dependence of charges on the $AgNO_3$ concentration. Each data point is the average of three replicates, and the error bars represent the standard deviations.

was observed. This is not surprising because the water droplet spreads more at the hydrophilic borosilicate glass surface. Although silanization of the borosilicate glass can produce dome-shaped droplets, the effect of droplet shape on the analyte diffusion time is not critical because of the large perimeter-to-area ratio of the microring electrode (an inherent advantage of a microring electrode over a microdisc electrode). From the chronoamperomogram in Figure 3A, only 85 s was needed for depleting all Ag^+ ions inside the spherical cap. A typical bulk electrolysis in a conventional electrochemical cell requires 60 min or so even with a large electrode area and constant and rapid stirring.[34] The area of our microring electrode (42 μm^2) is only ~10% of that of a microdisc electrode (408 μm^2) of the same radius (i.e., 11.4 μm). The fact that our electrolysis can be completed in less than 2 min suggests that the high diffusion rate and the small droplet volume largely offset the effect of the small electrode area. It is worth mentioning that during the Ag^+ reduction at the microring electrode, ion transfer (e.g., diffusion of a small amount of TBA^+ into the aqueous droplet) across the liquid/liquid interface must occur to maintain electroneutrality in the droplet. The total charge for Ag^+ reduction can be substituted into eq 2 to calculate the droplet volume. The volume calculated (1.42 nL) agrees extremely well with that using the width and height of the spherical cap estimated from the photomicrograph (1.45 nL). Figure 3B shows the stripping peaks recorded from droplets containing different Ag^+ concentrations, and the inset is a plot of the charges versus $[Ag^+]$. Linear regression of the plot yielded Q (nC) = 0.12 $[Ag^+]$ (μM) + 0.036 (R^2 = 0.995). Our results are reproducible as the relative standard deviations (RSD) are all below 14%, suggesting that highly comparable droplets can be dispensed. The detection limit of Ag^+, estimated from 3σ of the background, is 0.090 μM (9.7 ppb). Such a value corresponds to 0.13 fmol (14 fg) of Ag^+ in the 1.42-nL droplet and compares favorably to many other ASV assays conducted at microelectrodes in large sample volumes.[37−39] ASV in a single droplet at the microring electrode is more advantageous than that in a large solution at conventional-sized Hg drop or film electrodes,[40,41] as the latter does not exhaustively electrolyze the analytes. Carbon film-based interdigitated microelectrodes[42,43] or microcavities furnished with small gold stripes on the walls[15] have been used for ASV in small volumes. However, micro- to nanoliters of samples were still required to cover the working and auxiliary/reference electrodes. Reproducible analyses were also subject to variability in delivering solutions to the microcavities and affected by solution evaporation. Previously, we conducted ASV measurements of Cd^{2+} at an Hg-coated Pt microdisk electrode in a thin-layer flow cell.[44] Even with the combination of high preconcentration efficiency inherent in the amalgam formation and high sensitivity of fast scan voltammetry, the detection limit (190 fg) is still more than an order of magnitude higher than what we report here.

The microring electrode can also be used for flow-injection voltammetric analysis. In this mode the sample is back-loaded from a loop on a six-port rotary valve. Instead of remaining as a suspended droplet, the injected sample flows out of the capillary to an electrolyte solution. Figure 4 shows three

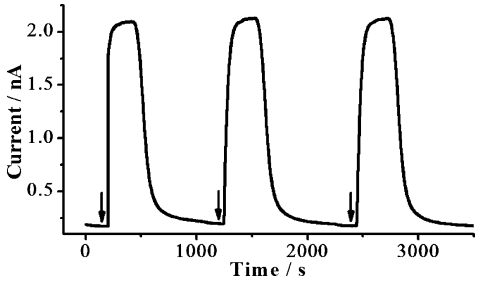

Figure 4. Flow-injection amperometric responses at a microring electrode corresponding to three injections of 5.0 mM $Ru(NH_3)_6^{3+}$ solution into a 0.1 M KCl solution. The flow rate was 5 μL/min and the electrode potential was held at −0.35 V vs Ag/AgCl. The arrows indicate the times of injections.

reproducible peaks corresponding to consecutive injections of a $Ru(NH_3)_6^{3+}$ sample into a flowing stream of KCl solution. The rapid rises and plateaus of the peaks indicate little dispersion of the sample concentration, a result of the small internal volume of the microring electrode/injector assembly. The small fused silica tubing interconnecting the valve and the microring electrode/injector assembly is inexpensive, small, and easily replaceable. This tubing helps prevent fine particulate matter in sample solution from clogging the microring electrode/injector assembly. Thus, we have demonstrated that the microring electrode/injector assembly is also adaptable for high-throughput electroanalysis. The easiness in connecting the microelectrode assembly to different sample injection systems and the ruggedness of the microring electrode (i.e., surface

dx.doi.org/10.1021/ac502316p | Anal. Chem. 2014, 86, 8037−8041

polishable and stable in organic solvents) are attractive for assaying different samples of small quantities.

CONCLUSION

A simple method for tightly sealing a gold microring electrode between tapered fused-silica capillary and encapsulating glass tubing is described. The size of the microring electrode can be easily altered and the electrode is robust and stable in organic solvent systems. Sample solutions can be either front-loaded using a microinjector or back-loaded using a rotary valve and an HPLC pump. The front-loading is particularly attractive for electroanalysis of samples of limited sizes, as single droplets of picoliter volumes can be conveniently formed and confined between the microring electrode and an immiscible liquid. The high electrolytic rate achieved in small droplets significantly reduces the analysis time, and the small ring size circumvents problems inherent in thin-layer cells consisting of large electrodes. ASV of Ag^+ resulted in a detection limit of 0.13 fmol (14 fg). Our approach is simpler than other methods based on a manipulator/positioner/injector for creating single droplets or nanofabricated wells for affording small cavities. These features are important for expanding the applications of microring electrodes.

ASSOCIATED CONTENT

Supporting Information

Additional information as noted in the text. This material is available free of charge via the Internet at http://pubs.acs.org/.

AUTHOR INFORMATION

Corresponding Author

*E-mail: fzhou@calstatela.edu.

Notes

The authors declare no competing financial interest.

ACKNOWLEDGMENTS

Partial support of this work by a National Science Foundation grant (NSF Grant 1112105), the National Key Basic Research Program of China (Grant 2014CB744502), and the NSF-CREST Program at California State University, Los Angeles (NSF Grant HRD-0931421) is gratefully acknowledged.

REFERENCES

(1) Montenegro, M. I.; Queirós, M. A.; Daschbach, J. L. *Microelectrodes: Theory and Applications*. NATO ASI Series E 197; Kluwer Academic Press: Dordrecht, The Netherlands, 1991.
(2) Bond, A. M. *Analyst* **1994**, *119*, 1R–21R.
(3) Ordeig, O.; del Campo, J.; Munoz, F. X.; Banks, C. E.; Compton, R. G. *Electroanalysis* **2007**, *19*, 1973–1986.
(4) Wightman, R. M. *Science* **2006**, *311*, 1570–1574.
(5) Bard, A. J.; Mirkin, M. V. *Scanning Electrochemical Microscopy*; Marcel Dekker: New York, 2001.
(6) Wightman, R. M.; Wipf, D. O. *Acc. Chem. Res.* **1990**, *23*, 64–70.
(7) Davies, P. W.; Brink, F., Jr *Rev. Sci. Instrum.* **1942**, *13*, 524–533.
(8) Mauzeroll, J.; Bard, A. J. *Proc. Natl. Acad. Sci. U.S.A.* **2004**, *101*, 7862–7867.
(9) Schulte, A.; Schuhmann, W. *Angew. Chem., Int. Ed.* **2007**, *46*, 8760–8777.
(10) Sun, P.; Laforge, F. O.; Abeyweera, T. P.; Rotenberg, S. A.; Carpino, J.; Mirkin, M. V. *Proc. Natl. Acad. Sci. U.S.A.* **2008**, *105*, 443–448.
(11) Takahashi, Y.; Shevchuk, A. I.; Novak, P.; Babakinejad, B.; Macpherson, J.; Unwin, P. R.; Shiku, H.; Gorelik, J.; Klenerman, D.; Korchev, Y. E.; Matsue, T. *Proc. Natl. Acad. Sci. U.S.A.* **2012**, *109*, 11540–11545.
(12) Venton, B. J.; Wightman, R. M. *Anal. Chem.* **2003**, *75*, 414 A–421 A.
(13) Lin, Y.; Trouillon, R. l.; Svensson, M. I.; Keighron, J. D.; Cans, A. S.; Ewing, A. G. *Anal. Chem.* **2012**, *84*, 2949–2954.
(14) Clark, R. A.; Hietpas, P. B.; Ewing, A. G. *Anal. Chem.* **1997**, *69*, 259–263.
(15) Vandaveer, W. R.; Fritsch, I. *Anal. Chem.* **2002**, *74*, 3575–3578.
(16) Troyer, K. P.; Wightman, R. M. *Anal. Chem.* **2002**, *74*, 5370–5375.
(17) Lawrence, N. S.; Jiang, L.; Jones, T. G.; Compton, R. G. *Anal. Chem.* **2003**, *75*, 2499–2503.
(18) Neugebauer, S.; Evans, S. R.; Aguilar, Z. P.; Mosbach, M.; Fritsch, I.; Schuhmann, W. *Anal. Chem.* **2004**, *76*, 458–463.
(19) Wei, C.; Bard, A. J.; Mirkin, M. V. *J. Phys. Chem.* **1995**, *99*, 16033–16042.
(20) Nakatani, K.; Sudo, M.; Kitamura, N. *Anal. Chem.* **2000**, *72*, 339–342.
(21) Nakatani, K.; Uchida, T.; Misawa, H.; Kitamura, N.; Masuhara, H. *J. Phys. Chem.* **1993**, *97*, 5197–5199.
(22) Yum, K.; Cho, H. N.; Hu, J.; Yu, M.-F. *ACS Nano* **2007**, *1*, 440–448.
(23) Girault, H.; Schiffrin, D. In *Electroanalytical Chemistry*; Bard, A. J., Ed.; Marcel Dekker: New York, 1989; Vol. *15*.
(24) Rodgers, P. J.; Amemiya, S. *Anal. Chem.* **2007**, *79*, 9276–9285.
(25) Rodgers, P. J.; Amemiya, S.; Wang, Y.; Mirkin, M. V. *Anal. Chem.* **2009**, *82*, 84–90.
(26) Li, Q.; Xie, S.; Liang, Z.; Meng, X.; Liu, S.; Girault, H. H.; Shao, Y. *Angew. Chem., Int. Ed.* **2009**, *48*, 8010–8013.
(27) Cope, D. K.; Tallman, D. E. *J. Electroanal. Chem.* **1990**, *285*, 85–92.
(28) Lee, Y.; Amemiya, S.; Bard, A. J. *Anal. Chem.* **2001**, *73*, 2261–2267.
(29) Macpherson, J. V.; Unwin, P. R. *Anal. Chem.* **1998**, *70*, 2914–2921.
(30) Macpherson, J. V.; Jones, C. E.; Unwin, P. R. *J. Phys. Chem. B* **1998**, *102*, 9891–9897.
(31) Macpherson, J. V.; Unwin, P. R. *Anal. Chem.* **1999**, *71*, 2939–2944.
(32) Walsh, D. A.; Fernández, J. L.; Mauzeroll, J.; Bard, A. J. *Anal. Chem.* **2005**, *77*, 5182–5188.
(33) Lee, Y.; Bard, A. J. *Anal. Chem.* **2002**, *74*, 3626–3633.
(34) Bard, A. J.; Faulkner, L. R. *Electrochemical Methods: Fundamentals and Applications*; John Wiley & Sons: New York, 2001.
(35) Dudko, O. K.; Szabo, A.; Ketter, J.; Wightman, R. M. *J. Electroanal. Chem.* **2006**, *586*, 18–22.
(36) Nakatani, K.; Uchida, T.; Misawa, H.; Kitamura, N.; Masuhara, H. *J. Electroanal. Chem.* **1994**, *367*, 109–114.
(37) Wehmeyer, K. R.; Wightman, R. M. *Anal. Chem.* **1985**, *57*, 1989–1993.
(38) Baranski, A. S.; Quon, H. *Anal. Chem.* **1986**, *58*, 407–412.
(39) Wong, D. K.; Ewing, A. G. *Anal. Chem.* **1990**, *62*, 2697–2702.
(40) Wang, J. *Stripping Analysis: Principles, Instrumentation, and Applications*; CVH Publishers: Deerfield Beach, FL, 1985.
(41) Wang, J. *Electroanalysis* **2005**, *17*, 1341–1346.
(42) Palchetti, I.; Laschi, S.; Mascini, M. *Anal. Chim. Acta* **2005**, *530*, 61–67.
(43) Nie, Z.; Nijhuis, C. A.; Gong, J.; Chen, X.; Kumachev, A.; Martinez, A. W.; Narovlyansky, M.; Whitesides, G. M. *Lab Chip* **2010**, *10*, 477–483.
(44) Zhou, F.; Aronson, J. T.; Ruegnitz, M. W. *Anal. Chem.* **1997**, *69*, 728–733.